Int. J. Heat Mass Transfer. Vol. 24, pp. 315–322
Pergamon Press Ltd. 1981. Printed in Great Britain

0017-9310/81/0201-0315 $02.00/0

MIXED CONVECTION IN AN ISOTHERMAL HORIZONTAL TUBE: SOME RECENT THEORIES

C. A. HIEBER
Sibley School of Mechanical and Aerospace Engineering, Cornell University, Ithaca, NY 14853, U.S.A.

(*Received* 14 *April* 1980 *and in revised form* 8 *August* 1980)

Abstract — Comparison is made between an earlier analysis by the author and more recent theoretical investigations of mixed convection in an isothermal horizontal tube. It is again substantiated that the primary parameter for determining the bulk-temperature rise under buoyancy-dominated conditions is given by the fourth root of the Rayleigh number divided by the Graetz number. The theory is shown to correlate existing data with an RMS deviation of $\simeq 8\%$ for water and 15% for ethyl alcohol and 80/20 glycerol water. Although derived for a large-Prandtl-number fluid, it is found that the theory can equally well describe available data in air.

NOMENCLATURE

a, pipe radius;
C_p, specific heat;
g, gravity;
Gr, Grashof number, $g\beta|\Delta T|a^3/\nu^2$;
k, thermal conductivity;
L, pipe length;
p, pressure;
Pr, Prandtl number, $\mu C_p/k$;
q_w, heat flux at wall;
r, radial coordinate;
Re, Reynolds number, Wa/ν;
T_a, average of bulk temperatures at inlet and outlet;
T_b, bulk temperature;
T_c, core temperature relative to T_b, see (2.11);
T_0, uniform temperature at inlet;
T_w, uniform wall temperature;
u, radial velocity component;
v, azimuthal velocity component;
V_B, $\equiv(\nu/a)\,(Gr/Pr)^{1/2}$;
$\tilde{V}_B$, $\equiv(\nu/a)\,(z/aRe)\,(Gr/Pr^{2/3})$;
w, axial velocity component;
W, average axial velocity;
z, axial coordinate.

Greek symbols

α, thermal diffusivity;
β, coefficient of volumetric thermal expansion;
δ, $\equiv\sqrt{(\lambda z)}$;
δ_B, $\equiv a/(GrPr)^{1/4}$;
ΔT, $\equiv T_w - T_0$;
ΔT_b, bulk temperature rise;
ε_1, $\equiv(z/aRe)^2(Gr/Pr^{1/3})$;
ζ, $\equiv(a-r)/\delta_B$;
λ, $\equiv\nu/W$, "viscous length";
μ, dynamic viscosity;
ν, kinematic viscosity;
ξ, $\equiv z/(aRePr)$;
ρ, fluid density;
σ, $\equiv(GrPr)^{1/4}\xi$;
ϕ, azimuthal coordinate measured from vertically downwards (upwards) in case of heated (cooled) wall;
χ, $\equiv(a-r)/\delta$;
ψ, streamfunction;
ω, see following (2.7).

Subscripts

a, evaluated at T_a;
B, buoyancy-induced;
c, core;
exp, experimental;
F, forced-flow induced;
L, evaluated at $z = L$;
w, evaluated at wall.

1. INTRODUCTION

ALTHOUGH it appears to have been the first theoretical analysis of mixed convection in an isothermal horizontal tube, and although it correlated much of the available data better than the best empirical correlations, [1] seems to have received a rather "mixed" response, at best. For example, (i) in their finite-difference investigation of this problem, Ou and Cheng [2] note the similarity between their own predictions and those in [1] but indicate that a direct comparison cannot be made since the entrance flow conditions are different in the two cases (in fact, the main result in [1] is independent of the entrance flow condition, and, as will be shown in Section 2, when the results in [2] are rescaled in terms of the variables in [1], the various curves in [2] collapse into a single curve which essentially coincides with the theoretical curve of [1]); (ii) in his detailed perturbation analysis of the entrance flow region for this problem, Yao [3] summarily dismisses the analysis in [1] on the basis that it neglects the interaction between the core flow and the boundary-layer flow (in fact, the analysis for the "near region" in [1] was concerned with following the effect of buoyancy upon the heat transfer and not upon the

flow structure of the core; nevertheless, Section 3 now indicates how the analysis in [1] could be extended to include the leading effect of buoyancy upon the core flow, thus serving as a large-Prandtl-number asymptote for the results in [3]); (iii) in their summary discussion of this problem area, admittedly with no claim of being comprehensive, Shah and London [4] cite only the empirical correlation developed in [5] (even though the theoretical result in [1] correlates the rather extensive data in [5–7] better than any of the empirical correlations developed in any of these investigations).

The purpose of the present paper, then, is to elucidate and further substantiate the theory developed in [1]. This is done on the one hand by showing in Sections 2 and 3 how [1] can be related to the results in [2] and [3], respectively. On the other hand, it is shown in Section 4 that a composite result, based upon the theory of [1] and the rescaled results from [2], correlates the data in [5–7] with an RMS deviation of 8% for water and 15% for ethyl alcohol and 80/20 glycerol water. In addition, it is found that although the theory has been derived for a large-Prandtl-number fluid, it can equally well describe the heat-transfer results in air reported in [8].

2. COMPARISON OF THE RESULTS OF OU AND CHENG [2] WITH [1]

Although the numerical simulation by Ou and Cheng [2] is for a fully-developed inlet velocity whereas the near-region analysis in [1] is for a uniform inlet velocity, the major results in [1], namely the expansions for the intermediate and far-intermediate regions, can still be applied when the inlet flow is fully developed. In this case, provided $Pr > 0(1)$ and $GrPr > 0(1)$, the bulk-temperature rise in the region

$$O\{(GrPr)^{-3/4}\} < \xi < O\{(GrPr)^{-1/4}\} \tag{2.1}$$

is given by the results in Section 2(d) of [1], namely

$$\Delta T_b = \Delta T \sum_{n=1}^{\infty} C_n \sigma^n \tag{2.2}$$

where, for $n = 1$–6,

$$C_n = 0.87052,\ -0.47363,\ 0.20615,\ -0.07851,\ 0.02734,\ -0.00892 \tag{2.3}$$

and σ (or "ε_3", in the notation of [1]) is defined as:

$$\sigma \equiv \frac{z}{aRe}\left(\frac{Gr}{Pr^3}\right)^{1/4} \equiv (GrPr)^{1/4}\xi \tag{2.4}$$

which, in effect, is the fourth root of the Rayleigh number divided by the Graetz number.

That is, according to the theory developed in [1], σ is the primary variable for determining the bulk-temperature rise for mixed convection in an isothermally heated or cooled horizontal tube. Accordingly, in making comparison with the finite-difference calculations of Ou and Cheng [2], it is appropriate to rescale their results in terms of σ. In this regard, it is noted that Fig. 7 of [2] presents results for $(\Delta T - \Delta T_b)/\Delta T$ vs $\xi/4$ (in present notation) for various values of $GrPr$, namely 5×10^3, 10^4, 5×10^4, 10^5, 5×10^5 and 10^6. A replotting of various points in terms of $\Delta T_b/\Delta T$ vs σ gives the results in Fig. 1. That is, the results for different $GrPr$ collapse into one curve which is well represented by the results of [1]. In particular, the solid curve in Fig. 1 corresponds to the first six terms in (2.2) whereas the dashed curve corresponds to an empirical extrapolation, namely

$$\frac{\Delta T_b}{\Delta T} = 0.543 + 0.315(\sigma - 1) - 0.132(\sigma - 1)^2 + 0.028(\sigma - 1)^3 \tag{2.5}$$

which was obtained in [1] for $1 \leqslant \sigma \leqslant 2.5$ based upon comparison with existing data.

The agreement indicated in Fig. 1 between the results in [1] and [2] is rather remarkable, typically being within a few per cent. Further, it is noted that the poorer agreement for the smaller $GrPr$ results at the smaller values of σ is due to the forced-convective effect of the near region where ξ is still the controlling parameter. On the other hand, although the forced convection will reappear as the dominant heat-transfer mechanism as ΔT_b approaches ΔT, with ξ again becoming the pertinent variable, the scaled results from [2] in Fig. 1 indicate that σ is still the controlling parameter when ΔT_b is as large as $\approx 98\%$ of ΔT.

At this point, it is suggested that the more casual reader skip to Section 4 since the remainder of this section and the following section are concerned with more detailed comparisons between [1] and [2] and between [1] and [3], respectively. In particular, in making comparison between [1] and [2], it should be noted that the theoretical result (2.2), from [1], is based upon a model in which the azimuthal velocity component is of order

$$V_B \equiv \frac{\nu}{a}\left(\frac{Gr}{Pr}\right)^{1/2} \tag{2.6}$$

in both the thermal boundary layer, which is of order $a/(GrPr)^{1/4}$ in thickness, and in the core. Further, it is assumed that the core is not thermally stratified, i.e. as the temperature rise in the core becomes of $O(\Delta T)$, the temperature variation across the core remains of order $\Delta T/(GrPr)^{1/4}$.

For comparison, it is noted that the results at $GrPr = 10^5$ in Fig. 6(a) of [2] indicate that the angular velocity, non-dimensionalized with respect to α/a, is as large as 100 to 200 in both the core and thermal boundary layer in the region $5 \times 10^{-4} \lesssim \xi/4 \lesssim 3 \times 10^{-3}$ ("z" in [2] corresponding to $\xi/4$, in present notation). This is to be compared with $V_B = (\nu/a)(Gr/Pr)^{1/2} = (\alpha/a)(GrPr)^{1/2} \simeq 300\,\alpha/a$, indicating that V_B is indeed the characteristic speed in this domain. On the other hand, the corresponding results for the temperature field in Fig. 3 of [2] indicate that the core does become thermally stratified but that this does not become significant until $\xi/4 \simeq 10^{-2}$, where, according

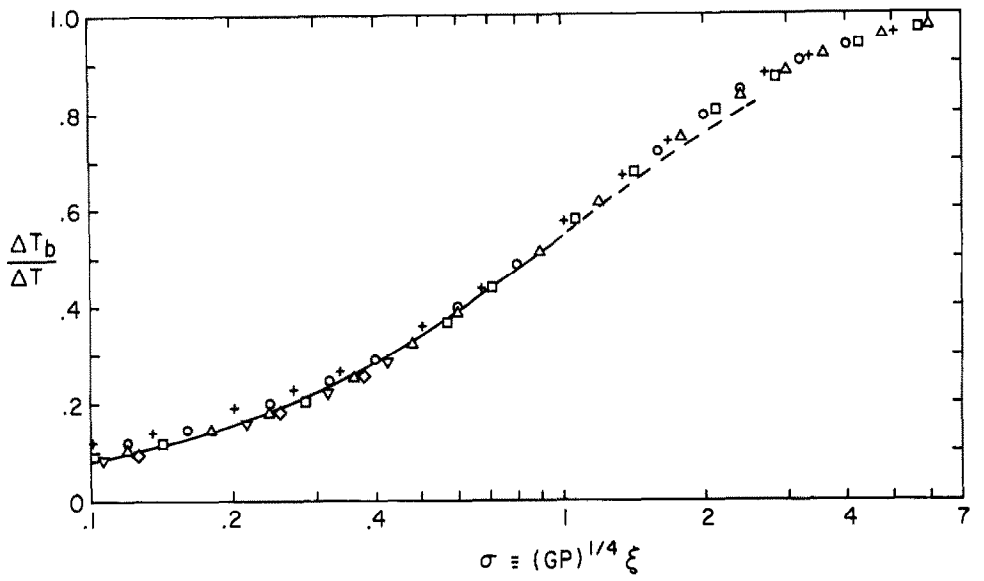

FIG. 1. Rescaled results from Fig. 7 of [2] for $GP = 5 \times 10^3$ (+), 10^4 (○), 5×10^4 (△), 10^5 (□), 5×10^5 (▽) and 10^6 (◇). Solid curve corresponds to first six terms in (2.2); dashed curve given by (2.5).

to Fig. 6(a), the secondary velocity in the core has already diminished to $\approx 40\,\alpha/a$. In this regard, it is noted that it is clear on physical grounds that thermal stratification cannot become significant until $\Delta T_b = O(\Delta T)$; further, by means of a global energy balance with q_w based upon $k\,\Delta T(GrPr)^{1/4}/a$, it follows that $\Delta T_b = O(\Delta T)$ where ξ is of order $(GrPr)^{-1/4}$ [i.e. $\sigma = O(1)$] which, for $GrPr = 10^5$, gives $\xi/4 \simeq .10^{-2}$.

The picture which therefore arises from the results in [2] is that, in agreement with the model in [1], the buoyancy-dominated structure is first characterized by a non-stratified core with angular velocities of $O(V_B)$ in both the core and thermal boundary layer. However, unlike the model in [1], the results in [2] indicate the development of significant thermal stratification in the core when ΔT_b becomes of $O(\Delta T)$. Accordingly, one would expect good agreement between [1] and [2] when $\Delta T_b/\Delta T$ is small. However, the fact that the non-stratified theory of [1] still describes the results in [2] when $\Delta T_b/\Delta T$ is as large as 54%, as shown in Fig. 1, indicates that stratification does not have such a drastic effect upon the global heat transfer. In fact, this point was already surmised in [1] where it was noted that, for the uniform-heat-flux case, the stratified solution of Siegwarth *et al.* [9] for the buoyancy-dominated, fully-developed flow region gives a circumferentially averaged Nusselt number which differs by only 10% from the corresponding non-stratified solution.

As a further illustration of the relationship between [1] and [2], it is noted that the results in [1] can be readily extended to a determination of the secondary velocity in the viscous core, corresponding to the situation in [2] prior to significant stratification. As noted in [1], the neglect of inertial effects in the core requires that $Gr < O(Pr)$. In this case, v_B and u_B in the core are related to a streamfunction, ψ_B, which is biharmonic and satisfies evident symmetry conditions along $\phi = 0, \pi$ together with the conditions

$$\psi_B = 0, \quad -\frac{\partial \psi_B}{\partial r} = V_B \omega^{1/2} \sin^{1/3}\phi\, f'(\infty) \text{ at } r = a \tag{2.7}$$

where $\omega \equiv \int_0^\phi \sin^{1/3} t\, dt$ (corresponding to "ξ" in [1]) and $f(\eta)$ corresponds to the similarity solution for the streamfunction in the inner layer, such that $f'(\infty) = 1.02136$, as given in (2.24) of [1]. That is, the inhomogeneous boundary condition in (2.7) corresponds to the non-zero asymptotic value of v_B at the edge of the inner layer.

A series solution for ψ_B can be expressed as

$$\psi_B = V_B a \sum_{n=1}^{\infty} c_n \left(\frac{r}{a}\right)^n \left(1 - \frac{r^2}{a^2}\right) \sin n\phi \tag{2.8}$$

where

$$c_n = \frac{f'(\infty)}{\pi} \int_0^\pi \omega^{1/2} \sin^{1/3}\phi \sin n\phi\, d\phi. \tag{2.9}$$

A resulting plot for $\psi_B/(V_B a)$, based upon the first ten terms in (2.8), is shown in Fig. 2. In particular, these results indicate that

$$(\psi_B)_{\max} \simeq 0.25 V_B a = 0.25 \frac{\nu}{a}\left(\frac{Gr}{Pr}\right)^{1/2} \times a = 0.25\alpha(GrPr)^{1/2} \tag{2.10}$$

where α is the thermal diffusivity. For comparison, it is noted that the results in Figs. 2 and 3 of Ou and Cheng [2] indicate a $\psi_{\max}$ of $\gtrsim 45\,\alpha$ and $70\,\alpha$, respectively, at $GrPr = 5 \times 10^4$ and 10^5 whereas (2.10) gives

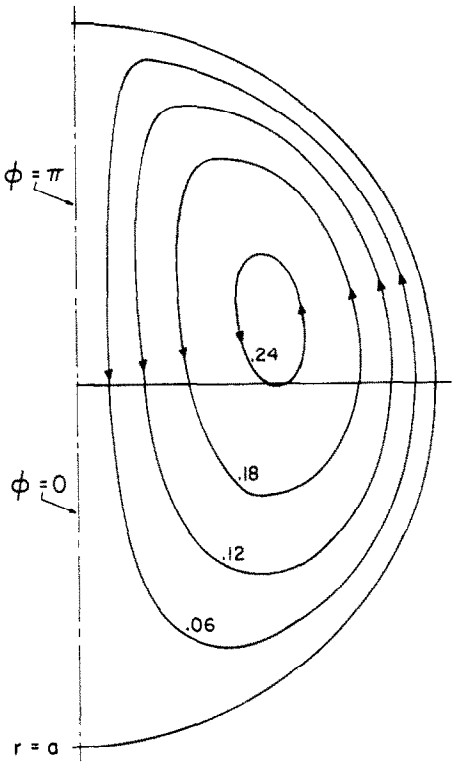

FIG. 2. Solution for $\psi_B/(V_B a)$ in viscous core as given by first ten terms in (2.8).

corresponding values of 56 α and 79 α, in reasonable agreement. That is, as discussed above, the calculations in [2] indicate that the maximum secondary flow in the core occurs prior to significant stratification, thus the good correlation of ψ_{max} with the present non-stratified theory. Further, in comparing the contours in Fig. 2 with these in Figs. 2 and 3 of [2], it should be noted that the plots in [2] are shown for the cooled-wall case whereas that in Fig. 2 of the current work is for the heated-wall case. Hence, the results in [2] indicate that, for the heated-wall case, the eye of the vortex will lie in the upper quadrant prior to stratification, in agreement with Fig. 2, but then become weaker and move into the lower quadrant as the thermal stratification becomes substantial.

Finally, it should be noted that the results in [2] at $GrPr = 10^5$ could be interpreted as indicating a rather limited overlap region in which there is $O(\Delta T)$ stratification in part of the core together with $O(V_B)$ secondary velocities [e.g. the region $10^{-3} \lesssim \xi/4 \lesssim 2 \times 10^{-3}$ where the results indicate significant stratification in the upper (lower) part of core for the heated (cooled) wall case]; it would then follow that the interaction between this secondary velocity and core temperature would give rise to a thermal-convection effect of order $V_B\,\Delta T/a = (\nu\,\Delta T/a^2)\,(Gr/Pr)^{1/2}$. For comparison, with q_w being of order $k\Delta T(GrPr)^{1/4}/a$, it follows that $w\,dT_b/dz$ is on the order of $(\nu\,\Delta T/a^2)\,(Gr^{1/4}/Pr^{3/4})$, which is seen to be smaller than the above convection term by order $(GrPr)^{-1/4}$. Indeed, this is the very reason that, for the fully-developed buoyancy-dominated region in the uniform-heat-flux case, one cannot have $O(\Delta T)$ stratification together with $O(V_B)$ secondary velocities, as was shown by Siegwarth *et al.* [9]. In the present case, however, since the stratification is developing with z, we have that the temperature distribution in the core is of the form

$$T(r,\theta,z) = T_b(z) + T_c(r,\theta,z). \tag{2.11}$$

Hence, by requiring that $w\partial T_c/\partial z$ balance the convection due to the secondary flow, it follows that $\partial T_c/\partial z$ should be on the order of $(\Delta T/(aPrRe))\,(GrPr)^{1/2}$. In particular, from Fig. 5 of [2] it is noted that, e.g. at $r/a = 0.6$ and $\phi = \pi$, the change in $T_b + T_c$ between $\xi/4 = 10^{-3}$ and 2×10^{-3} is $\simeq 0.27\,\Delta T$ whereas, from Fig. 7 of [2], the corresponding change in T_b is seen to be $\simeq 0.03\,\Delta T$; hence, for this r/a and ϕ, the average value of $\partial T_c/\partial z$ between the above two values of ξ is approximately

$$\frac{\partial T_c}{\partial z} \simeq \frac{0.24\,\Delta T}{(10^{-3})(4aPrRe)} = 60\frac{\Delta T}{aPrRe}$$

where the 60 is to be compared with $(10^5)^{1/2} \simeq 300$, indicating marginal agreement. In fact, the thermal convection due to the secondary flow has been overestimated in the above since the secondary velocity at $\xi/4 = 2 \times 10^{-3}$ and $r/a = 0.6$, $\phi = \pi$ is only a small fraction of V_B, as can be seen from the streamline pattern in Fig. 3 of [2] together with the above discussion of Fig. 6(a).

Nevertheless, the above indicates at least a tendency for $\partial T_c/\partial z$ to be on the order of $(\Delta T/(aPrRe))\,(GrPr)^{1/2}$. In turn, noting that the buoyancy arising from T_c in the core can only be balanced hydrostatically, it follows that the associated pressure, p_c, will be on the order of $\rho g\beta a T_c$. Hence, with the axial gradient of p_c being balanced by viscous diffusion of w, it follows that the corresponding induced axial velocity component will be such that

$$\mu\frac{\Delta w_c}{a^2} \sim \rho g\beta a\frac{\partial T_c}{\partial z} \sim \frac{\rho g\beta a\Delta T}{aPrRe}(GrPr)^{1/2},$$

i.e. Δw_c will be on the order of $W(GrPr)^{3/2}/(RePr)^2$, where this effect should be most evident in the top (bottom) of the core in the case of a heated (cooled) wall. Further, it is noted that this pressure gradient would tend to be adverse in this region of the core. [It should also be pointed out that the above result for Δw_c is the same as obtained by Siegwarth *et al.* [9] for the uniform-heat-flux case except for an additional $(GrPr)^{1/4}$ in the numerator due to $\partial T_c/\partial z$ being order $(GrPr)^{1/4}$ larger than dT_b/dz.] Accordingly, it seems that the simplification in [2] of neglecting any change in w due to buoyancy would require that $(GrPr)^{3/2}/(RePr)^2$ be small. However, at least as regards heat-transfer predictions, it appears that this constraint is unnecessarily restrictive since the experimental data cited in Section 4, which is well described

by the theory of [1] and [2], corresponds to values of the above parameter as large as 4000. Even in terms of the less restrictive criterion of [9], it is noted that the data corresponds to values of $(GrPr)^{5/4}/(RePr)^2$ as large as 125.

3. RELATING THE WORK OF YAO [3] TO [1]

Both [1] and [3] employ asymptotic expansion techniques to analyze mixed convection in an isothermally heated or cooled horizontal pipe. In the former investigation, the expansion is for large Prandtl number whereas the latter is for Pr of $O(1)$; in both instances, the velocity is assumed to be uniform at the entry. Accordingly, the leading-order forced-flow velocity boundary layer is given in both cases by the well-known Blasius solution for flow over a flat plate, with a boundary-layer thickness of order $\delta \equiv \sqrt{(\lambda z)}$ where $\lambda \equiv \nu/W$. In [1], due to the large-Prandtl-number assumption, the forced-flow thermal boundary layer is of order $\delta/Pr^{1/3}$ in thickness, being imbedded within the Blasius boundary layer and being described by a suitably scaled Leveque solution. This forced-flow temperature distribution results in a buoyancy term which induces an angular velocity of $O(\tilde{V}_B)$, where

$$\tilde{V}_B \equiv \frac{\nu}{a}\left(\frac{z}{aRe}\right)\frac{Gr}{Pr^{2/3}}.$$

In turn, this buoyancy-induced flow (more specifically, the radial component thereof) convects the forced-flow temperature field and thus gives rise to a buoyancy-induced temperature which, in like manner, induces further flow. As shown in [1], this expansion for the buoyancy-induced flow and temperature proceeds in powers of ε_1, where

$$\varepsilon_1 \equiv \left(\frac{z}{aRe}\right)^2 \frac{Gr}{Pr^{1/3}}.$$

In [3], on the other hand, due to $Pr = O(1)$, the thermal boundary layer is of $O(\delta)$ in thickness and the associated leading-order buoyancy-induced angular velocity is of order

$$\frac{\nu}{a}\left(\frac{z}{aRe}\right)Gr,$$

which is seen to agree with $\tilde{V}_B$ if Pr is $O(1)$. Rather than proceeding in powers of ε_1, as in [1], the interest in [3] is with determining the resulting buoyancy-induced flow in the core. If this had been done in [1], it would have required first determining the behavior of the buoyancy-induced flow in the velocity boundary layer, as is shown below.

In particular, in the notation of Section 2(a) in [1], we would have

$$w_F\frac{\partial v_{B_1}}{\partial z} + u_F\frac{\partial v_{B_1}}{\partial r} = \nu\frac{\partial^2 v_{B_1}}{\partial r^2} \tag{3.1}$$

and

$$\frac{\partial v_{B_1}}{a\partial\phi} + \frac{\partial u_{B_1}}{\partial r} = 0 \tag{3.2}$$

subject to the conditions that

$$u_{B_1} = 0, \quad v_{B_1} = 2.0401\,\tilde{V}_B \sin\phi \quad \text{at } \chi = 0$$
$$v_{B_1} \sim 0 \quad \text{as } \chi \to \infty \tag{3.3}$$

where $\chi \equiv (a - r)/\delta$ and the inhomogeneous condition in (3.3) arises from matching the asymptotic behavior of v_{B_1} at the outer edge of the thermal boundary layer, as given in (2.8) of [1]. However, following Yao [3], the situation for $(\ )_{B_1}$ in the velocity boundary layer is more complicated due to the inertial term $u_{B_1}\,\partial w_F/\partial r$ which gives rise to a w_{B_1} of $O(\tilde{V}_B z/a)$ and which, therefore, contributes a term to (3.2). That is, with w_{B_1} being governed by

$$u_{B_1}\frac{\partial w_F}{\partial r} + w_{B_1}\frac{\partial w_F}{\partial z} + w_F\frac{\partial w_{B_1}}{\partial z} + u_F\frac{\partial w_{B_1}}{\partial r} = \nu\frac{\partial^2 w_{B_1}}{\partial r^2} \tag{3.4}$$

subject to the conditions

$$w_{B_1} = 0 \quad \text{at } \chi = 0, \quad w_{B_1} \sim 0 \quad \text{as } \chi \to \infty \tag{3.5}$$

and $\partial w_{B_1}/\partial z$ being added to (3.2), it follows that an appropriate representation is given by

$$v_{B_1} = \tilde{V}_B\,\Phi_1' \sin\phi \tag{3.6}$$

$$u_{B_1} = \tilde{V}_B\frac{\delta}{a}(\Phi_1 + \tfrac{5}{2}\Phi_2 - \tfrac{1}{2}\chi\Phi_2')\cos\phi \tag{3.7}$$

$$w_{B_1} = \tilde{V}_B\frac{z}{a}\Phi_2' \cos\phi \tag{3.8}$$

with $\Phi_1(\chi)$ being governed by

$$\left.\begin{aligned}\Phi_1''' + \tfrac{1}{2}F\Phi_1'' - F'\Phi_1' = 0\\ \Phi_1(0) = 0 = \Phi_1'(\infty), \quad \Phi_1'(0) = 2.0401\end{aligned}\right\} \tag{3.9}$$

and $\Phi_2(\chi)$ by

$$\left.\begin{aligned}\Phi_2''' + \tfrac{1}{2}F\Phi_2'' - 2F'\Phi_2' + \tfrac{5}{2}F''\Phi_2 = -F''\Phi_1\\ \Phi_2(0) = 0 = \Phi_2'(0) = \Phi_2'(\infty)\end{aligned}\right\} \tag{3.10}$$

where $F(\chi)$ corresponds to the well-known Blasius solution, governed by

$$F''' + \tfrac{1}{2}FF'' = 0; \quad F(0) = 0 = F'(0),$$
$$F'(\infty) = 1. \tag{3.11}$$

Numerical solution of the above results in

$$\Phi_1''(0) = -1.1066, \quad \Phi_1(\infty) = 2.4507 \tag{3.12}$$

and

$$\Phi_2''(0) = 0.5855, \quad \Phi_2(\infty) = 1.8249. \tag{3.13}$$

In particular, the non-zero value of $\Phi_2''(0)$ indicates that w_{B_1} will be of $O(\tilde{V}_B Pr^{-1/3} z/a)$ in the thermal boundary layer, thus contributing a term of $O(\tilde{V}_B Pr^{-1/3}/a)$ to the continuity equation and hence justifying its neglect in

determining v_{B_1} and u_{B_1} in the inner layer, as was done in [1]. On the other hand, as $\chi \to \infty$,

$$u_{B1} \sim C_1 \tilde{V}_B \frac{\delta}{a} \cos\phi \tag{3.14}$$

where $C_1 = 2.4507 + \frac{5}{2}(1.8249) = 7.0130$. For comparison, it is noted that, in the present terminology, Yao obtains

$$u_{B_1} \sim 2^{3/2}\beta_2 (Pr^{2/3}\tilde{V}_B)\frac{\delta}{a}\cos\phi \quad \text{as} \quad \chi \to \infty \tag{3.15}$$

with $\beta_2 = 0.3158$ for $Pr = 10$, thus giving a value for $2^{3/2}\beta_2 Pr^{2/3}$ of 4.146. This poor agreement with the above value for C_1 can, in fact, be attributed to the presence of higher-order terms in the large-Prandtl-number expansion. In particular, by extending the analysis to these higher-order terms, it can be shown that

$$C_1 = 7.0130 - 7.2220\, Pr^{-1/3} + O(Pr^{-1}) \tag{3.16}$$

such that, as applied to $Pr = 10$, the first two terms in (3.16) result in a value of 3.661, which is seen to agree within about 10% of the value of 4.146 from Yao, as would be expected from the omitted $O(Pr^{-1})$ term in (3.16).

Accordingly, for the large-Pr limit, one can make direct use of the core results obtained by Yao [3]. In the present notation, this becomes (for large z/a):

$$u_{B_1} = C_1 \tilde{V}_B \frac{\delta}{a}\cos\phi \tag{3.17}$$

$$v_{B_1} = -C_1 \tilde{V}_B \frac{\delta}{a}\sin\phi \tag{3.18}$$

$$w_{B_1} = \tfrac{3}{2} C_1 \tilde{V}_B \frac{\delta}{z}\frac{r}{a}\cos\phi \tag{3.19}$$

$$p_{B_1} = -\tfrac{3}{2} C_1 \rho W \tilde{V}_B \frac{\delta}{z}\frac{r}{a}\cos\phi \tag{3.20}$$

such that the buoyancy-induced velocity in the r–ϕ plane is in the vertical direction (downwards in the heated-wall case, upwards in the cooled-wall case) and of magnitude $C_1 \tilde{V}_B \delta/a$.

In summary, it is noted that the "near region" expansion in [1] and the expansion in [3] require that both ε_1 and δ/a be small. That is, the expansions break down when either ε_1 becomes $O(1)$, i.e. $z/aRe = O(Pr^{1/6}/Gr^{1/2})$, indicating that the natural convection has become a leading-order heat-transfer effect, or $\delta/a = O(1)$, i.e. $z/aRe = O(1)$, indicating that the viscous boundary layer has merged along the centerline. Accordingly, which of these conditions is met first depends upon whether $Gr > O(Pr^{1/3})$ or $Gr < O(Pr^{1/3})$. In the former case, the thermal boundary layer is buoyancy dominated in the region $z/aRe > O(Pr^{1/6}/Gr^{1/2})$ with its thickness being of order $a/(GrPr)^{1/4}$ and the associated angular velocity being of order $(v/a)\,(Gr/Pr)^{1/2}$. On the other hand, if $Gr < O(Pr^{1/3})$ then the thermal boundary layer remains forced-flow dominated in the region $z/aRe > 0(1)$ but is now imbedded within Poiseuille flow, in leading approximation, with the thickness of the thermal layer being of order $a(z/aRePr)^{1/3}$. In this case, the natural convection will remain a smaller-order effect until the region where $z/(aRe) = O(Pr^{1/4}/Gr^{3/4})$. However, if this region corresponds to $z/(aRe) > O(Pr)$, i.e. if $Gr < O(Pr^{-1})$, then the forced-flow-dominated temperature field will have already become fully developed ($T \sim T_w$), indicating that natural convection remains a smaller-order effect throughout if $GrPr < O(1)$, as might be expected.

In particular, then, for the case $Gr < O(Pr^{1/3})$, the results in (3.17) and (3.18) imply that, in the region $z/(aRe) = 0(1)$, the secondary velocities in the (viscous) core will be of the same order as in the thermal layer. By further extrapolation, the results of Yao suggest that the eventual buoyancy-dominated structure will also be characterized by significant secondary velocities in the core. Such a result is seen to be compatible with the numerical results of Ou and Cheng [2], preceding significant thermal stratification, as discussed in the previous section.

Finally, it should be noted that the analysis of Yao [3] represents the first attempt, for the present configuration, at predicting the effects of natural convection upon the axial pressure gradient, an issue which is not addressed by either [1] or [2]. Although no simple task, it appears that this problem will be most readily resolved by extending the finite-difference calculation of [2] to include the axial force balance. In this regard, it is noted that the recent work by Abdelmeguid and Spalding [10] indicates that such a numerical capability is at hand; however, even in their calculation, which is for the developing turbulent mixed convection in a uniform-heat-flux pipe (horizontal, vertical or inclined), it is found necessary to neglect the radial and ϕ dependence of the axial pressure gradient.

4. COMPARISON WITH EXPERIMENTAL RESULTS

Shown in Fig. 3 is a comparison between the theoretical results from [1] and [2] and the experimental results of Oliver [6], Brown and Thomas [5] and Depew and August [7]. In particular, the solid and dashed curves in Fig. 3 are the same as in Fig. 1, being based upon equations (2.2) and (2.5), respectively; on the other hand, the long-short curve in Fig. 3 corresponds to the following least-square fitting of the results from [2], as shown in Fig. 1 for $\sigma > 0.7$:

$$\frac{\Delta T_b}{\Delta T} = \sum_{n=0}^{5} D_n \sigma^n, \quad 0.7 \lesssim \sigma \lesssim 6.0 \tag{4.1}$$

where

$$D_n = 0.00369,\ 0.80669,\ -0.31435,\ 0.066911,\ -0.0073590,\ 0.00032559 \tag{4.2}$$

for $n = 0 - 5$. Following the standard Sieder–Tate empiricism, the data points have been processed by

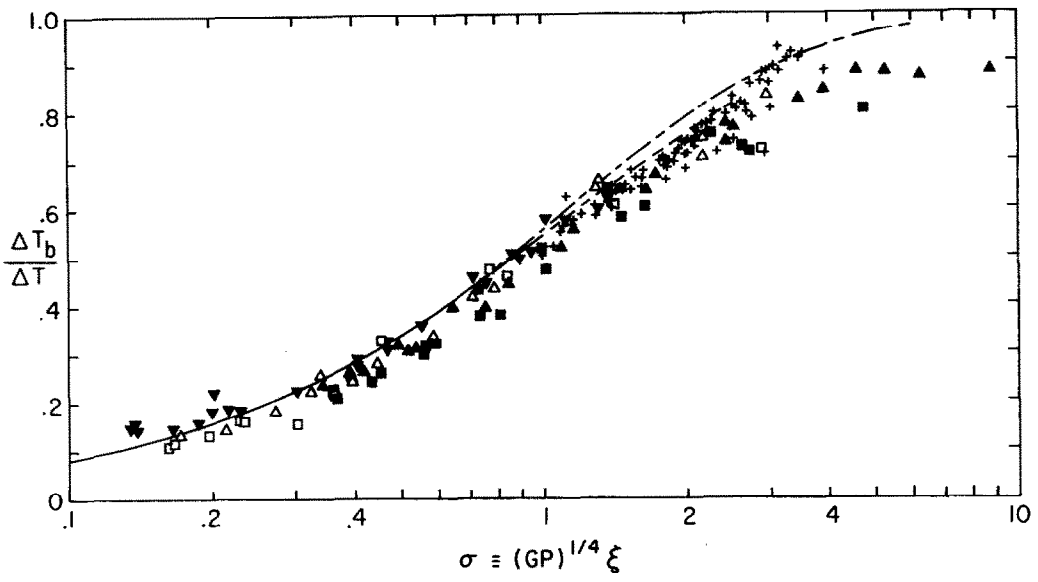

FIG. 3. Comparison of theory with data of Oliver [water (▲), ethyl alcohol (■) and 80/20 glycerol water (▼)], Brown & Thomas [water (+)] and Depew & August [water (△) and ethyl alcohol (□)]. Solid curve is based upon (2.2), dashed curve upon (2.5) and long-short curve upon (4.1). The abscissa and ordinate for data are, respectively, σ_L and $(\Delta T_b/\Delta T)_{exp}\,(\mu_w/\mu_a)^{0.14}$.

evaluating all physical properties at the average bulk temperature, $T_a = T_0 + \frac{1}{2}\Delta T_b$, and multiplying the measured $\Delta T_b/\Delta T$ by the factor $(\mu_w/\mu_a)^{0.14}$. In general, it is seen that the data compare quite well with the theory. In fact, relative to a composite result based upon (2.2) for $\sigma < 0.7$ and upon (4.1) for $0.7 \leqslant \sigma \leqslant 6.0$, the RMS deviation of the various data shown in Fig. 3 (excluding the two points beyond 6.0) is as follows: 9% (▲), 15% (■), 15% (▼), 7% (+), 8% (△) and 14% (□).

On the basis of the above, it would seem that the present theory can fairly well describe buoyancy-dominated convective heat transfer for large-Prandtl-number fluids in isothermal horizontal tubes. That is, provided $(GrPr)^{1/4}$ and Pr are large, and σ lies in the range shown in Fig. 3, the bulk-temperature rise would be expected to correlate well with the composite curve based upon (2.2) and (4.1). In particular, for the experimental points shown in Fig. 3, $(GrPr)^{1/4}$ ranges from as low as ≈ 7 in the glycerol–water data of [6] to as high as ≈ 45 in the water results from [5]. Further, Pr ranges from as low as ≈ 4 in [5] to as high as ≈ 500 for the glycerol–water data in [6]. The data include both the heated-wall ([6]) and cooled-wall ([5–7]) cases and both fully-developed ([6] and [7]) and uniform ([5]) inlet-velocity conditions.

It is indicated in [1], however, that the oil data of Kern and Othmer [11] do not correlate well with the theory. In this case, $(GrPr)^{1/4}$ ranged from ≈ 17 to 120 with Pr lying between ≈ 35 and 1700. Except for the data for which $(GrPr)^{1/4} < 30$, the results in [11] tend to lie 30–50% below the theory. Although one complicating factor in this case is the possibility of an unstable flow associated with the larger $(GrPr)^{1/4}$ values (note: Gr is here based upon tube radius)—in fact, Kern and Othmer noted that their results were highly susceptible to external disturbances (see p. 526 of [11])—the fact that the present laminar theory *over*predicts the heat-transfer rate seems to militate against the possibility of turbulence. Another cause of discrepancy with the theory could be a large value of $(GrPr)^{5/4}/(RePr)^2$ which, according to [9] and the discussion at the end of Section 2 above, might lead to a significant change in the flow structure due to a modulation in the axial velocity arising from buoyancy effects upon the axial pressure gradient. In this regard, it is noted that the data in [11] include runs for which the above parameter is as large as 2000; however, there are also runs which exhibit the same significant deviation from the present theory but for which the above parameter is much smaller than one. (For comparison, this parameter gets as large as 125 for the data shown in Fig. 3.) Accordingly, the discrepancy with the data in [11] remains unresolved although one contributing factor may be the severe heating conditions, $T_w - T_0$ ranging between 125 and 220°C, with the associated large variations in the oil viscosity. This effect will be considered further in a separate investigation.

In closing, it is interesting to note that although the present theory has been based upon the assumption of a large Prandtl number, an analysis of the corresponding experimental data obtained by Jackson *et al.* [8] in air indicates that (2.2) and (4.1) seem to correlate the results in this case also. That is, with a T_w of 100°C, a detailed analysis of the results presented in Fig. 3 of [8] indicates that T_0 was ≈ 33°C and $(GrPr)^{1/4} \approx 28$ (in present notation) with the bulk-temperature measurements lying roughly 10% below (2.2) and (4.1). A more

detailed presentation of these and other experimental results will be given in a future communication.

REFERENCES

1. C. A. Hieber and S. K. Sreenivasan, Mixed convection in an isothermally heated horizontal pipe, *Int. J. Heat Mass Transfer* **17**, 1337–1348 (1974).
2. J. W. Ou and K. C. Cheng, Natural convection effects on Graetz problem in horizontal isothermal tubes, *Int. J. Heat Mass Transfer* **20**, 953–960 (1977).
3. L. S. Yao, Free-forced convection in the entry region of a heated straight tube, *J. Heat Transfer* **100**, 212–219 (1978).
4. R. K. Shah and A. L. London, *Laminar Flow Forced Convection in Ducts*, p. 412. Academic Press, New York (1978).
5. A. R. Brown and M. A. Thomas, Combined free and forced convection heat transfer for laminar flow in horizontal tubes, *J. Mech. Engng Sci.* **7**, 440–448 (1965).
6. D. R. Oliver, The effect of natural convection on viscous-flow heat transfer in horizontal tubes, *Chem. Engng Sci.* **17**, 335–350 (1962).
7. C. A. Depew and S. E. August, Heat transfer due to combined free and forced convection in a horizontal and isothermal tube, *J. Heat Transfer* **93**, 380–384 (1971).
8. T. W. Jackson, J. M. Spurlock and K. R. Purdy, Combined free and forced convection in a constant temperature horizontal tube, *A.I.Ch.E.Jl* **7**, 38–41 (1961).
9. D. P. Siegwarth, R. D. Mikesell, T. C. Readal and T. J. Hanratty, Effect of secondary flow on the temperature field and primary flow in a heated horizontal tube, *Int. J. Heat Mass Transfer* **12**, 1535–1552 (1969).
10. A. M. Abdelmequid and D. B. Spalding, Turbulent flow and heat transfer in pipes with buoyancy effects, *J. Fluid Mech.* **94**, 383–400 (1979).
11. D. Q. Kern and D. F. Othmer, Effect of free convection on viscous heat transfer in horizontal tubes, *Trans. Am. Inst. Chem. Engrs* **39**, 517–555.

CONVECTION MIXTE DANS UN TUBE HORIZONTAL ET ISOTHERME: QUELQUES THEORIES RECENTES

Résumé — Une comparaison est faite entre une précédente analyse par l'auteur et des études théoriques plus récentes sur la convection mixte dans un tube isotherme et horizontal. Il est encore dégagé que le paramètre pour déterminer l'élévation de la température moyenne sous des conditions dominées par les forces d'Archimède est donné par la racine quatrième du nombre de Rayleigh divisé par le nombre de Graetz. La théorie s'accorde avec les données existantes dans une moyenne quadratique de 8% pour l'eau, de 15% pour l'alcool éthylique et le mélange 80/20 de glycerol et d'eau. Bien que celà soit obtenu pour un fluide à grand nombre de Prandtl, on montre que la théorie peut aussi bien décrire convenablement les données connues pour l'air.

GEMISCHTE KONVEKTION IN EINEM ISOTHERMEN HORIZONTALEN ROHR: EINIGE NEUERE THEORIEN

Zusammenfassung—Es wird ein Vergleich zwischen einer früheren Analyse des Autors und neueren theoretischen Untersuchungen der gemischten Konvektion in einem isothermen horizontalen Rohr durchgeführt. Dabei bestätigt sich wieder, daß der wesentliche Parameter zur Bestimmung der Zunahme der Mitteltemperatur unter von Auftrieb bestimmten Bedingungen durch die vierte Wurzel aus der Raleigh-Zahl, dividiert durch die Graetz-Zahl, gegeben ist. Es wird gezeigt, daß durch die Theorie vorliegende Daten mit einer mittleren quadratischen Abweichung von 8% für Wasser und von 15% für Äthylalkohol und 80/20 Glyzerin–Wasser–Mischungen wiedergegeben werden. Obwohl die Theorie für Fluide mit großer Prandtl-Zahl abgeleitet wurde, zeigte sich, daß sie gleichermaßen verfügbare Daten für Luft beschreiben kann.

СМЕШАННАЯ КОНВЕКЦИЯ В ИЗОТЕРМИЧЕСКОЙ ГОРИЗОНТАЛЬНОЙ ТРУБЕ. РЯД НОВЫХ ТЕОРИЙ

Аннотация — Проведено сравнение между методом, ранее предложенным автором, и более поздними теоретическими исследованиями смешанной конвекции в изотермической горизонтальной трубе. Еще раз показано, что основной параметр, описывающий рост объемной температуры в условиях преобладания сил выталкивания, определяется корнем четвертой степени из отношения чисел Релея и Гретца. Предлагаемый метод обобщает имеющиеся данные с точностью до 8% для воды и 15% для этилового спирта и раствора глицерина в воде в соотношении 80/20. Несмотря на то, что использовались данные для жидкости с большим числом Прандтля, предлагаемый метод хорошо описывает и имеющиеся данные для воздуха.